Supporting Information

A Robust Strategy for Crafting $Li_5Cr_7Ti_6O_{25}$@CeO_2 Composites as High-Performance Anode Material for Lithium-Ion Battery

Jie Mei, [a] Ting-Feng Yi, [a,b]* Xin-Yuan Li, [a] Yan-Rong Zhu, [a] Ying Xie,[b,*] Chao-Feng Zhang[*]

[a] *School of Chemistry and Chemical Engineering, Anhui University of Technology, Maanshan, Anhui 243002, People's Republic of China*

[b] *Key Laboratory of Functional Inorganic Material Chemistry, Ministry of Education, School of Chemistry and Materials Science, Heilongjiang University, Harbin 150080, People's Republic of China*

[c] *School of Chemistry and Chemical Engineering, Hefei University of Technology, Hefei, Anhui 230009, People's Republic of China*

E-mail: tfyihit@163.com (Dr. Ting-Feng Yi)

E-mail: xieying@hlju.edu.cn (Dr. Ying Xie).

E-mail: czhang@hfut.edu.cn (Dr. Chao-Feng Zhang).

1. $Li_5Cr_7Ti_6O_{25}$ and CeO_2-coated $Li_5Cr_7Ti_6O_{25}$ material preparation

$Li_5Cr_7Ti_6O_{25}$ and CeO_2-coated $Li_5Cr_7Ti_6O_{25}$ materials were prepared by a solid-state method. Li_2CO_3 (AR, ≥99.0%), Cr_2O_3 (AR, 99.0%), and anatase-phase TiO_2 (AR, 99.0%) were used as the raw materials. Excessive Li (3 wt%) was provided to compensate for the volatilization of lithium during the high temperature sintering. All raw materials are mixed and ball-milled. The high-energy ball milling processes were carried out at a constant speed of 350-400 rpm and a processing time of 3-5 h. After the ball milling process, the remaining alcohol medium was evaporated and the gained powders were subsequently dried at 100-120 °C for 8-10 h. The mixed raw materials were calcined at 450 °C for 4 h in air to gain the precursor. Then, the precursor and CeO_2 was ball-milled with alcohol as the medium for about 3-5 h. At last, the precursors were sintered at 850 °C for 12 h in a flowing air atmosphere to gain $Li_5Cr_7Ti_6O_{25}$ and CeO_2-coated $Li_5Cr_7Ti_6O_{25}$ powders.

2. Battery preparation and electrochemical characterizations

The half-cell comprises an electrode and a lithium metal negative electrode separated by a porous polypropylene separator. The slurry was prepared by blending the obtained powder, super P carbon, and PVDF (polyvinylidene fluoride) dissolved in NMP (1-Methyl-2-pyrrolidinone) with a weight ratio of 8:1:1. The slurry mentioned above was pasted onto a Cu foil by a doctor blade technique, and then dried at 110 °C for 10 h in vacuum drying oven. The average loading of active material is 2.0 mg cm^2. The CR 2025 coin-type cells were assembled in an Ar-filled glove box by using 1 M $LiPF_6$ in DMC: EC (1:1 in volume) as electrolyte. Electrochemical impedance spectroscopy (EIS) was measured by a CHI 760C

electrochemical work station over a frequency range from 0.01 Hz to10 kHz, and the potentiostatic signal amplitude is 5 mV. Cyclic voltammetry (CV) test was carried out on a CHI 1000C electrochemical work station in a voltage range between 1 and 2.5 V, and the scanning rate is 0.1 mV s^{-1}.

3. **Nomenclature for equations (1) and (2)**

T the absolute temperature

A the surface area of the electrode

F the Faraday constant

n the number of electrons per molecule during oxidation

R the gas constant

σ the Warburg factor

C_{Li} the concentration of lithium ion

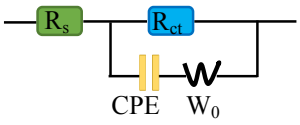

Figure S1 The equivalent circuit diagram used to fit EIS before cycling

*R*s represents the solution resistance caused by the electrolyte at high frequency intercept. The semicircle in the high frequency region corresponds to the charge transfer resistance (*R*ct), and the linear tail at the low frequency region (*W*) are ascribed to the solid-phase diffusion of Li^+ ion.

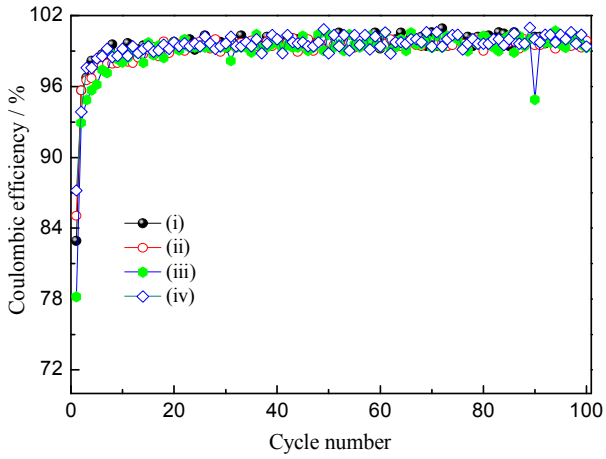

Figure S2 Coulombic efficiency of pristine $Li_5Cr_7Ti_6O_{25}$ and $Li_5Cr_7Ti_6O_{25}$@CeO_2 electrodes at 5 C charge-discharge rate. (i) 0 CeO_2, (ii) 3 wt.% CeO_2, (iii) 5 wt.% CeO_2, and (iv) 10 wt.% CeO_2. Both the charge rate and discharge rate are completely the same.

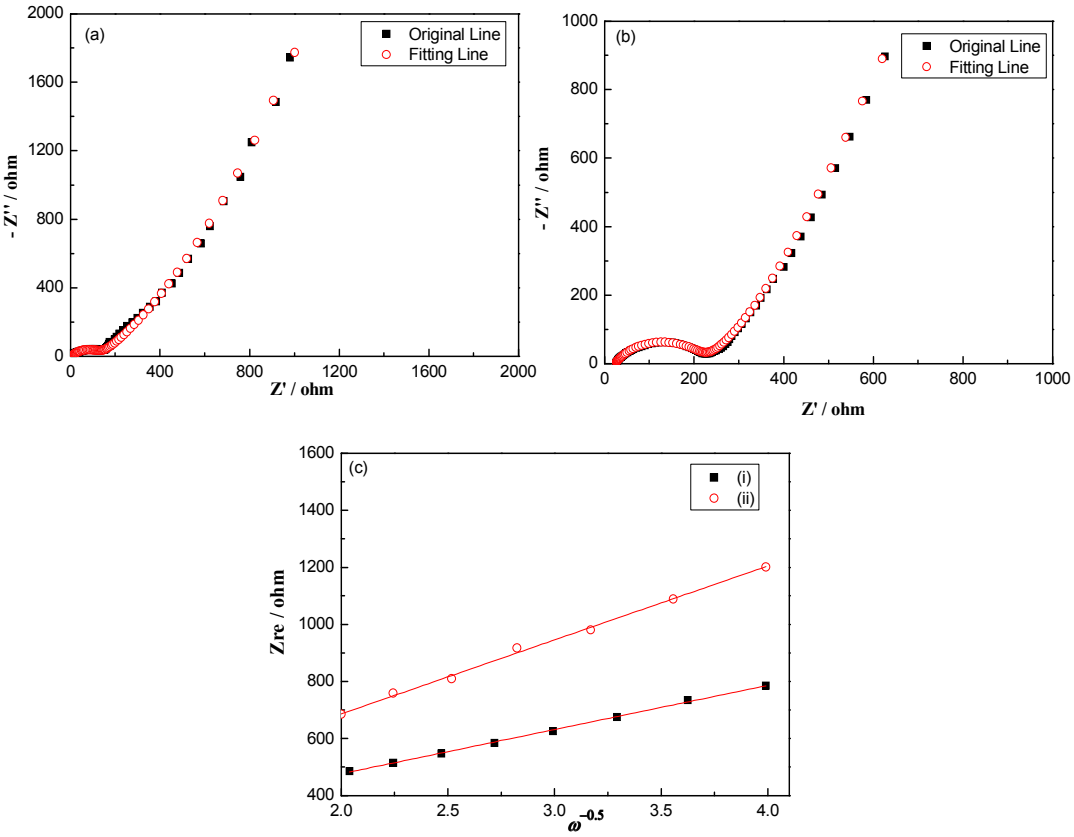

Figure S3. EIS patterns and fitted Nyquist plots of (a) $Li_5Cr_7Ti_6O_{25}$ and (b) $Li_5Cr_7Ti_6O_{25}$@CeO_2 (3 wt %) after 20 cycles at 0.2 C rate charged to 2.5 V, (c) corresponding correlation between Z_{re} and $\omega^{-0.5}$ at the low frequency range of (i) $Li_5Cr_7Ti_6O_{25}$@CeO_2 (3 wt %) and (ii) $Li_5Cr_7Ti_6O_{25}$

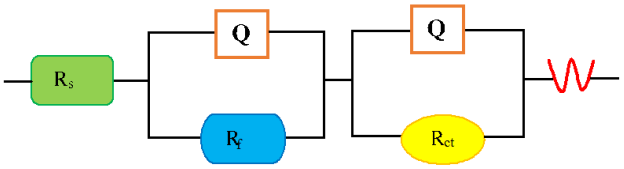

Figure S4 The equivalent circuit diagram used to fit EIS after cycling

In the equivalent circuit, the two depressed semicircles observed at high and mid frequencies are attributed to the resistance (R_f) and constant phase elements (CPE1, Q) of the SEI film, and the charge-transfer resistance (R_{ct}) and constant phase elements (CPE2, Q) of the electrode, respectively. The slope line at low frequencies corresponds to the Warburg impedance (Z_w), which is related to lithium ion diffusion within the particles.

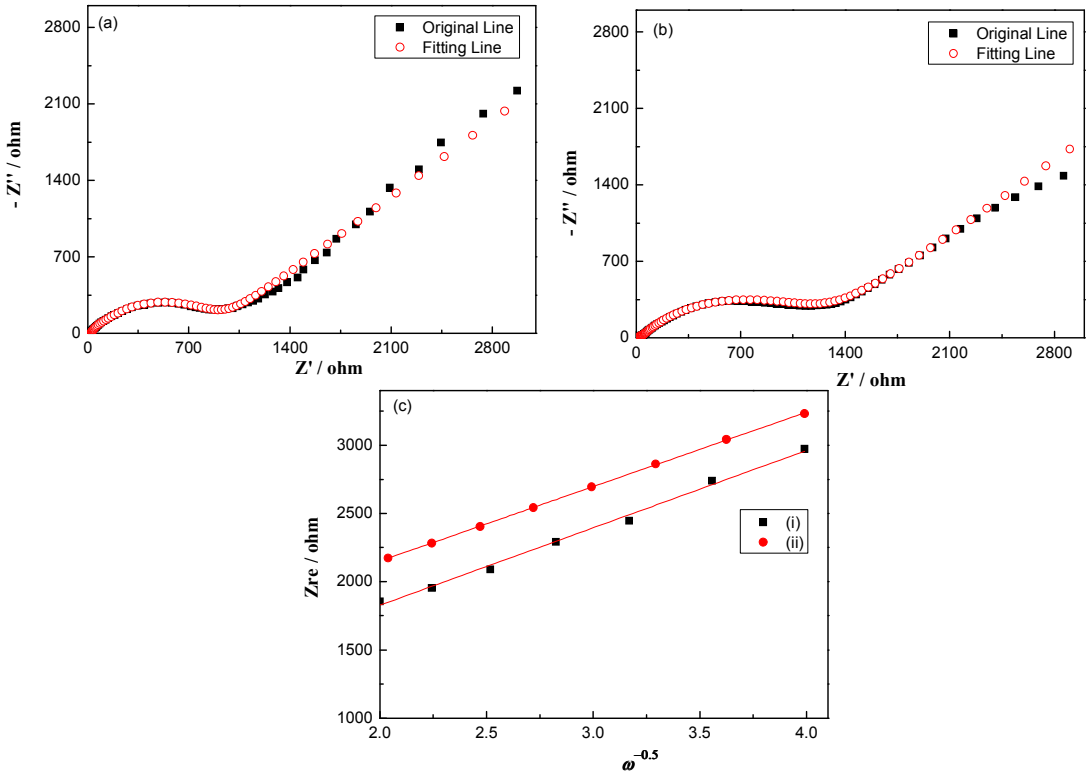

Figure S5. EIS patterns and fitted Nyquist plots of (a) $Li_5Cr_7Ti_6O_{25}$ and (b) $Li_5Cr_7Ti_6O_{25}$@CeO_2 (3 wt %) after 20 cycles at 0.2 C rate discharged to 1 V, (c) corresponding correlation between Z_{re} and $\omega^{-0.5}$ at the low frequency range of (i) $Li_5Cr_7Ti_6O_{25}$@CeO_2 (3 wt %) and (ii) $Li_5Cr_7Ti_6O_{25}$

Table S1 Fitted results of $Li_5Cr_7Ti_6O_{25}$@CeO_2 (0, 3, 5 and 10 wt %)

	0 wt %	3 wt %	5 wt %	10 wt %
R_s/ Ω	26.58	22.47	14.31	17.5
R_{ct} / Ω	757.2	182	106.5	68.6
D_{Li} / $cm^2 \cdot s^{-1}$	8.63×10^{-17}	1.32×10^{-16}	1.24×10^{-16}	8.55×10^{-17}

Table S2. Comparison of discharge capacity between $Li_5Cr_7Ti_6O_{25}$@CeO_2 (3 wt %) in this work and previously reported $Li_4Ti_5O_{12}$ electrodes prepared by solid-state method.

Electrodes	**Synthesis method**	**Rate capacity (mAh g^{-1})**	**Refs**
$Li_4Ti_5O_{12}$	Solid state	100 @5C	41
$Li_4Ti_5O_{12}$	Solid state	<70 @5C	42
A- $Li_4Ti_5O_{12}$	Solid state	<60 @5C	43
$Li_4Ti_5O_{12}$	Solid state	90 @4C	44
$Li_4Ti_5O_{12}$	Solid state	125 @0.2C	45
F-doped $Li_4Ti_5O_{12}$	Solid state	90 @5C	46
Mg-doped $Li_4Ti_5O_{12}$	Solid state	80 @5C	46
Fe-doped $Li_4Ti_5O_{12}$	Solid state	90 @5C	47
$Li_4Ti_5O_{12}$/graphene	Solid state	70 @5C	48
$Li_4Ti_5O_{12}$/C	Solid state	<120 @5C	49
$Li_4Ti_5O_{12}$/Li_2TiO_3	Solid state	100 @5C	50
$Li_4Ti_5O_{12}$	Sol-gel	65.7 @5C	51

$Li_4Ti_5O_{12}$	glycine-nitrate auto-combustion	93 @5C	52
$Li_4Ti_5O_{12}$	high-energy ball milling assisted solid-state	105 @1C (100 cycles)	53
$Li_5Cr_7Ti_6O_{25}@CeO_2$ (3 wt %)	Solid state	104.6@5 C 144.2@0.2 C 116 @1 C (100 cycles)	This work

Table S3 Fitted results of pristine $Li_5Cr_7Ti_6O_{25}$ and $Li_5Cr_7Ti_6O_{25}@CeO_2$ (3 wt %) after 20 cycles at 0.2 C rate at charge state and discharge state

	$Li_5Cr_7Ti_6O_{25}$ Charge state	$Li_5Cr_7Ti_6O_{25}@CeO_2$ Charge state	$Li_5Cr_7Ti_6O_{25}$ Discharge state	$Li_5Cr_7Ti_6O_{25}@CeO_2$ Discharge state
R_{ct} / Ω	123.2	117	36.6	12.4
D_{Li} / cm^2 s^{-1}	1.14×10^{-15}	3.18×10^{-15}	2.38×10^{-16}	2.57×10^{-16}